CAPACITIVE BASED CMOS-MEMS MICROACTUATOR FOR BIOMEDICAL APPLICATION

by

Marfarahain bt. Samuri

Final report submitted in partial fulfilment of the requirements for the

Bachelor of Engineering (Hons)

(Electrical & Electronics Engineering)

MAY 2011

Universiti Teknologi PETRONAS
Bandar Seri Iskandar
31750 Tronoh
Perak Darul Ridzuan

CERTIFICATION OF APPROVAL

CAPACITIVE BASED CMOS-MEMS MICROACTUATOR FOR BIOMEDICAL APPLICATION

by

Marfarahain bt. Samuri

Final report submitted to the
Electrical & Electronics Engineering Programme
Universiti Teknologi PETRONAS
in partial fulfilment of the requirement for the
BACHELOR OF ENGINEERING (Hons)
(ELECTRICAL & ELECTRONICS ENGINEERING)

Approved by,

(Dr.Mohd Haris bin Mohd Khir)

UNIVERSITI TEKNOLOGI PETRONAS

TRONOH, PERAK

May 2011

CERTIFICATION OF ORIGINALITY

This is to certify that I am responsible for the work submitted in this project, that the original work is my own except as specified in the references and acknowledgements, and that the original work contained herein have not been undertaken or done by unspecified sources or persons.

MARFARAHAIN SAMURI

ABSTRACT

The purpose of this project is to design electrostatic microactuator for biomedical application using CMOS and MEMS. The technology of microelectromechanical system (MEMS) is widely used in many daily applications such as aerospace Microsystems, biomedical applications, consumer electronic devices and so on. Specifically in biomedical applications, the experimentation always related to a macro meter objects manipulation. Due to that constraint, the tools that being used are also in macro meter-sized. Therefore, basically this project implements a micro actuator with an integrated capacitive force sensor which can be used in biomedical applications in handling cells and micron-size objects. An actuator for macro-size objects is already in market and it is not suitable to be used to the small cells like micron-cells. In my research, I had determined that there are several actuation principles of different types of gripper which are electrostatic, electromagnetic, electro thermal and electro osmotic. The problem where the procedure of handling the active cells must be taken seriously now can be solved with the invention of the grippers. In order to design the structure of this device, certain requirements should be taken into considerations. This project will improve the design for microactuator by applying electrostatic principles. The device then simulated in MATLAB to find other parameters needed for the microgripper. The performance of this device will be determined by its sensitivity for gripping the Hela cells. The device can be operated with 58V of actuator voltage supply and produced 9.9238 μN to have displacement of 1 μm. The results show that the device can be used with low voltage and able to be used for cell manipulations.

TABLE OF CONTENTS

CERTIFICATION i

ABSTRACT iii

LIST OF FIGURES vi

LIST OF TABLES viii

CHAPTER 1: INTRODUCTION 1

1.1 Background of Study 1

1.2 Problem Statement 4

1.3 Objectives 5

1.4 Scope of Study 5

1.5 Feasibility Project 6

CHAPTER 2: LITERATURE REVIEW 7

CHAPTER 3:	**METHODOLOGY**	15
CHAPTER 4:	**MICROACTUATOR DESIGN**	18
CHAPTER 5:	**RESULTS AND DISCUSSION**	25
	4.1 Simulation Results of the Optimized Structure	25
	4.2 Simulation Results of the Optimized Process	30
CHAPTER 6:	**CONCLUSIONS AND RECOMMENDATIONS** .	35
	5.1 Conclusions & Recommendations . .	35
REFERENCES	. . . .	36
APPENDICES	. . . .	43
	APPENDIX I : MATLAB CODING . . .	43

LIST OF FIGURES

Figure 1	CMOS Static RAM	7
Figure 2	Magnetic Microgripper using MEMS technology	9
Figure 3	CMOS-MEMS Accelerometer in 3-axis	10
Figure 4	Electrostatic force between two surfaces with different potentials	12
Figure 5	A curved electrostatic actuator	12
Figure 6	Hela cell structure	14
Figure 7	Project flow diagram	15
Figure 8	The input-output relation	16
Figure 9	Comb finger illustration (top view)	19
Figure 10	Springs attachment	20
Figure 11	2-Dimension of electrostatic microactuator structure	22
Figure 12	3-Dimension of Electrostatic microactuator	22
Figure 13	Graph of Electrostatic Force versus Voltage	26
Figure 14	Graph Displacement versus Electrostatic Force	27
Figure 15	Graph Displacement versus Voltage	28
Figure 16	Dynamic in time response function	29
Figure 17	Graph of Displacement versus Electrostatic Force (N increase)	30
Figure 18	Graph of Displacement versus Voltage with increasing N	31
Figure 19	Dynamic system of microactuator with increasing damping ratio, *b*	32

Figure 20 Dynamic system of microactuator with decreasing constant, k 33

LIST OF FIGURES

Table 1	Desired microactuator output	18
Table 2	Dimension of the electrostatic microactuator	23
Table 3	Parameters of the device	25
Table 4	Optimized parameters	34

CHAPTER 1: INTRODUCTION

1.1 Background

Micro actuator can be defined as a microscopic servomechanism that supplies and transmit a measured amount of energy for the operation of another mechanism or system [1]. It is based on three-dimensional mechanical structures with very small dimensions which are produced with the help of lithographic procedures and non-isotropic etching techniques. For an actuator-like displacement, the most different principles of force generation are used, such as the bimetal effect, piezo effect, shape memory effect and electrostatic forces [2].

Micro-electro-mechanical systems or MEMS are small integrated devices or systems that combine electrical and mechanical components. They range in size from sub-micrometer (or sub-micron) level to the millimetre level and can be any number, from a few to millions, in a particular system. MEMS extend the fabrication techniques developed for the integrated circuit industry to add mechanical elements such as beams, gears, diaphragms, and springs to devices [3]. The necessity to control multiple MEMS electrostatic actuators devices becoming an important issue for a variety of applications like aerospace microsystems [4], biomedical systems like automatic DNA samplers [5], consumer electronic systems like ink jet printers [6], video display projectors like Digital Light Processor (DLP), inkjet-printer cartridges, accelerometers, miniature robots, microengines, locks, inertial sensors, microtransmissions, micromirrors, micro actuators, optical scanners, fluid pumps, transducers, pressure and flow sensors. New applications are emerging as the existing technology is applied to the miniaturization and integration of conventional devices.

MEMS are, in their most basic forms, diminutive versions of traditional electrical and mechanical devices - such as valves, pressure sensors, hinged mirrors, and gears with dimensions measured in microns - manufactured by techniques similar to those used in fabricating microprocessor chips. The first MEMS products were developed in the 1960s, when accurate hydraulic pressure sensors were needed for aircraft. Such devices were further refined in the 1980s when implemented in fuel-injected car engines to monitor intake-manifold pressure. In the late 80s, MEMS accelerometers for car airbags were developed as a less expensive, more reliable, and more accurate replacement for a conventional crash sensor. Taking the spotlight today are optical MEMS (also known as Micro-Opto-Electro-Mechanical Systems, or MOEMS), primarily micro-mirrors, which are used as digital light processors in video projectors and as switches in optical network equipment.

After extensive development, today commercial MEMS - also known as Micro System Technologies (MST), Micro Machines (MM), or M3 (MST, MEMS & MM) have proven to be more manufacturable, reliable and accurate, dollar for dollar, than their conventional counterparts. However, the technical hurdles to attain these accomplishments were often costly and time-consuming, and current advances in this technology introduce newer challenges still. Because this field is still in its infancy, very little data on design, manufacturing processes, or reliability are common or shared [7].

In biomedical application such as for cell manipulation purposes which is the field of interest in this work, different types of micro gripper have been developed using various actuation principles which can be summarized as follows:

- Electromagnetic
- Thermal
- Phase-change
- Electro osmotic

- Electrostatic

These actuators can perform various operations such as grasping, pushing, pulling, positioning, orienting, and bending with nanometer precision [8]. For example, micro actuators have been demonstrated to grasp and bond carbon annotates (CNTs) (as small as 1–3 nm in diameter) onto atomic force microscope (AFM) probe tips (tip diameter <10 nm) for high-resolution, high-aspect ratio imaging [9]; to manipulate and handle fragile 300 nm thin transmission electron microscope (TEM) lamella [10]; and to precisely probe and separate biological cells/tissues [11,12]. While these examples demonstrate the potential of micro actuators to perform nanomanufacturing tasks, the future need to assemble 3D heterogeneous nanocomponents with a high degree of repeatability, accuracy, thermal stability, reliability, and throughput presents new challenges and requires further advances in research [13].

By internalize some materials from the journals, an electrostatic actuator was identified as the most suitable alternative for this project due to several reasons such as low power consumption, small in sizes, and less complex circuitry connection. An electrostatically driven micro gripper is reported in [14]. The gripper is fabricated from single crystal silicon using an SOI process. Comb drives are used as actuators in [15] for micro tweezers application. A capacitor is broadly defined as two conductors that can hold opposite charges. In this project, we use parallel plates that use the principle of a capacitor in order to let the gripper open its jaw to start gripping cells. It can be used as either a sensor or an actuator to perform the same functions. If a distance and relative position between two conductors change as a result of applied stimulus, the capacitance value would be changed. This forms the basis of capacitive (or electrostatic) sensing of positions. On the other hand, if a voltage (or electric field) were applied across two conductors, an electrostatic force would develop between these two objects. This is defined as electrostatic actuation.

1.2 Problem Statement

The culture practised in daily life does influence the level of our health. Excessive carbon consumed and genetics are some of the reasons why people easily exposed to cancer. Due to the increasing number of patients suffer for cancer disease, the researchers take this opportunity to create a vaccine of Hela cell. By experimenting the characteristics of Hela cell, the researchers faced a few problems in terms of medical instruments availability in manipulating the active cells and micron-objects size which are complex in handling. In biomedical applications, micro-electro-mechanical systems (MEMS) technology is widely used to increase and upgrade the availability of natural mechanism other than to ease the work energy. In order to manipulate the micrometer-sized objects, a miniaturized gripper with end-effectors on the size-scale should be used to help in minimizing the error of results of the experiment. In cell manipulation, the gripper itself may harm or affect the handled specimens such as life cycle of the cells, biomedical calculations and chemical reaction. Therefore, in designing a microactuator, some criteria should be followed in order to suit the cell manipulated. A gripper designed should suitable for the characteristics of manipulation cell in order not to directly or indirectly harm the cells physically.

1.3 Objectives

The objectives of this project are:

- To understand the basic principles of electrostatic actuators.
- To design the structure of capacitive based CMOS-MEMS Microactuators for biomedical application (Hela cell manipulation).
- To determine the device performance using MATLAB.

1.4 Scope of Study

1.4.1 Understanding CMOS-MEMS microactuator

The overall concept, technology and theoretical of electrostatic-based CMOS-MEMS microactuator needs to be understand before proceeding with the task of designing the structure of the device.

1.4.2 Design CMOS-MEMS microactuator for biomedical applications

Using certain CMOS technology, a microactuator will be design that meets the specified technical specifications.

1.4.3 Microactuator Characterization using MATLAB

Besides on paper design, microactuator structure design will be evaluated and characterized using MATLAB.

1.5 Feasibility of Project

In terms of technically feasibility, the knowledge learned in Microelectronics can be applied in completing this project. Some fundamentals of Silicon characteristic and fabrication process is used to design the structure in related software.

CHAPTER 2

LITERATURE REVIEW

2.1. CMOS

Complementary metal oxide semiconductor (CMOS) technology is prominently used for constructing integrated circuit in microprocessors, microcontroller, static RAM and also in other digital logic circuitry. The improved technologies were used for more than thirty years such as the transistors manufactured nowadays are 20 times faster and occupy less than 1% of the area of those built 20 years age [16].

Figure 1. CMOS Static RAM

Static RAM is one of the examples of CMOS technology that was widely used. It is a place in a computer where the operating system, application programs, and data in current use are kept so that they can be quickly reached by the computer's processor. RAM is much faster to read from and write to than the other kinds of storage in a computer, the hard disk, floppy disk, and CD-ROM. However, the data in RAM stays there only as long as your computer is running. When you turn the computer off, RAM loses its data. When you turn your computer on again, your operating system and other files are once again loaded into RAM, usually from your hard disk.

Two important characteristics of CMOS devices are high noise immunity and low static power consumption. More important, CMOS processes and variants have come to dominate due to the existence of many CMOS foundries, thus the vast majority of modern integrated circuit manufacturing is utilizing CMOS processes [17]. Significant power is only drawn when the transistors in the CMOS device are switching between on and off states. Consequently, CMOS devices do not produce as much waste as other forms of logic, for example transistor-transistor logic (TTL) or NMOS logic. CMOS also allow a high density of logic functions on a chip.

The phrase "metal–oxide–semiconductor" is a reference to the physical structure of certain field-effect transistors, having a metal gate electrode placed on top of an oxide insulator, which in turn is on top of a semiconductor material. Aluminum was once used but now the material is polysilicon.

2.2. Micro-electro-mechanical Systems (MEMS)

Micro-electro-mechanical systems (MEMS) are small devices fabricated by microelectronics manufacturing techniques. These microsystems also contain physical interfaces to their surrounding world, such as moving parts or sensing functions other than purely electrical. Some MEMS may not have moving parts and can be made from plastic, glass and dielectric materials. The name comes from the typical feature size being in the micro meter (μm) range. The operating principle of MEMS is based on frequency variation devices involving resonant structures and microelectronics. Frequency varying elements involve resonating beam cantilevers, diaphragms and other resonant structures. There are many applications where MEMS devices are used, for example pressure sensors, accelerometers, bio/chemical sensors, micro relays and switches. Commercially successful examples are hard disk heads, inkjet nozzles and airbag sensors [18].

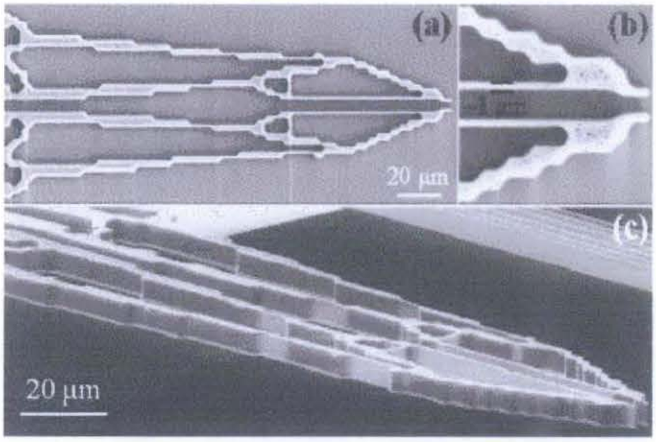

Figure 2. Magnetic Microgripper using MEMS technology

Figure 2 shows a magnetic based microgripper using MEMS technology. This type of microgripper is one of the biomedical instruments in cell manipulation using magnetic principle in handling. The concept of working is when there are magnetic reaction happened, there will result in displacement at the end of the gripper.

Production of MEMS devices involves micromachining and various specific processes such as deposition, etching, lithographic and chemical. MEMS components can be manufactured using very large-scale integration (VLSI) processing techniques. The fabrication of MEMS involves a modified integrated circuit (IC) technology involving a stress-controlled material process. These micro fabrication techniques have been honed to maximize device yield and microelectromechanical systems (MEMS) capitalize on these semiconductor micro fabrication tools to create miniature systems that meld electrical and mechanical functions. Miniaturization brings with it the benefits of smaller devices that cost less, require less power and incorporate greater functionality. The use of microsystems in biomedical applications holds the promise of improving patient care in a minimally invasive manner while simultaneously reducing health care costs.

2.2.1 CMOS-MEMS

Fusion of microelectromechanical systems (MEMS) technology with complementary metal-oxide semiconductor (CMOS) LSI technology is a promising way to develop highly functional devices beyond CMOS scaling. We have been developing the integrated CMOS-MEMS technology that fabricates MEMS devices on a silicon wafer. The integrated CMOS-MEMS technology features miniaturization, which leads to a thinner, a more high-functionality, high accuracy, mass-production, not only obtaining high functionality of CMOS circuitry and higher performance of MEMS devices. Not to mention its monolithically capability with circuits in the same substrates further increase device performance and sensitivity [19].

One example of technology using CMOS-MEMS is accelerometers for game devices and/or automotive vehicles [20]. Figure 3 shows how the technology was fabricated into a user-friendly device.

Figure 3. CMOS-MEMS Accelerometer in 3-axis

2.3. MEMS Actuation Methods

Using MEMS technology for microactuator, there are several principles that exist in some applications. There are magnetic actuation, piezoelectric actuation, thermal actuation and electrostatic actuation [21].

- *Magnetic*: Force is induced by a magnetic field application to actuate a magnetic material. This actuation mechanism is easy to implement at microscale, but an order of magnitude reduction in the device length induces a four orders of magnitude reduction in forces.
- *Piezoelectric*: A piezoelectric material converts electrical power into mechanical power via a crystallographic deformation. When there is a potential difference between two opposite surfaces, it changes its structure causing shortening, according to the electric field polarity.
- *Thermal*: Joule effect and materials deformation due to thermal expansion are the principle mechanism for this type of actuation. With careful choice of material and geometry, large displacements and forces can be obtained.
- *Electrostatic*: A Coulomb force is a surface density force applied by an electrostatic field created between two parallel conductor plates with different polarity.

For this project, the microactuator with electrostatic based method is emphasized. Electrostatic actuation is widespread in MEMS because its flexibility combinations and simplicity. In addition, this actuation mechanism is a surface volume phenomenon and scaling down the device dimensions enhances its effects. Other than that, the advantage such as simple fabrication process, less power consumption, and utilizes small area for the structure are the reason why electrostatic actuation is best designed for the biomedical applications.

2.4. Electrostatic Driven Micro Actuators

Many MEMS switches use electrostatic actuation [22]. The principle behind this actuation mode is the use of parallel plate of a capacitor that produced electrostatic forces developed between elements with a potential difference. Such forces are a result of Coulomb's law for the force between charged particles. Electrostatic concept based on parallel plate is illustrated below:

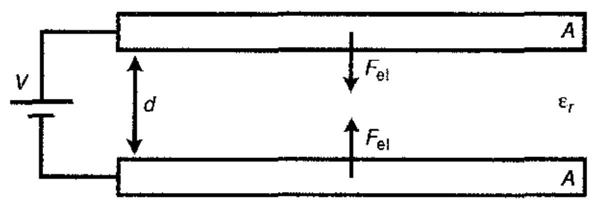

Figure 4. Electrostatic force between two surfaces with different potentials

A simple example is shown in Figure 4. There are two parallel surfaces of area A. They are separated by a distance d and the medium between them has a dielectric constant ε_r. Then the potential difference, V between them creates an attractive (electrostatic) force of

$$F_e = \frac{1}{2}\varepsilon_0\varepsilon_r A\frac{V^2}{d^2}. \quad (2.1)$$

The electrostatic force from Equation (2.1) can thus be used to actuate MEMS structures, as shown in Figure 4. The fixed electrode attracts the moving cantilever electrode, making it to bend towards the fixed electrode [23].

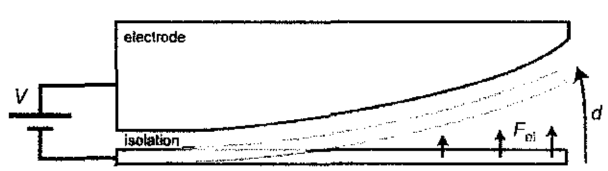

Figure 5. A curved electrostatic actuator

A simple electrostatic actuator in Figure 5 often referred to as curved-electrode. If an isolation layer is used between the fixed electrode and the cantilever electrode, the cantilever can roll along the curved surface. The rest of this thesis concerns with the effects of electrostatic actuators used for micro cell manipulation.

2.5. Hela Cell

In biomedical applications of microsystems fall broadly into two categories diagnostic and therapeutic systems. Diagnostic applications include DNA diagnostics [24-26], systems on chips [27-29] and cell [30] and molecule [31] sorting. Therapeutic systems include drug and gene delivery [32-38], tissue augmentation/ repair [39], micro/minimally invasive surgical systems [40, 41] and biocapsules [42, 43].

Medical researchers use laboratory-grown human cells to learn the intricacies of how cells work and test theories about the causes and treatment of diseases. The cell lines they need are "immortal"—they can grow indefinitely, be frozen for decades, divided into different batches and shared among scientists. In 1951, a scientist at Johns Hopkins Hospital in Baltimore, Maryland, created the first immortal human cell line with a tissue sample taken from a young black woman with cervical cancer. Those cells, called HeLa cells, quickly became invaluable to medical research—though their donor remained a mystery for decades.

In order to help the researchers to manipulate the cell, a micro actuator is designed specifically for this Hela cell. Henrietta's cells were the first immortal human cells ever grown in culture. This opportunity made the researchers to initiate a cell manipulation. They were essential to developing the polio vaccine. They went up in the first space missions to see what would happen to cells in zero gravity. Many scientific landmarks since then have used her cells, including cloning, gene mapping and in vitro fertilization.

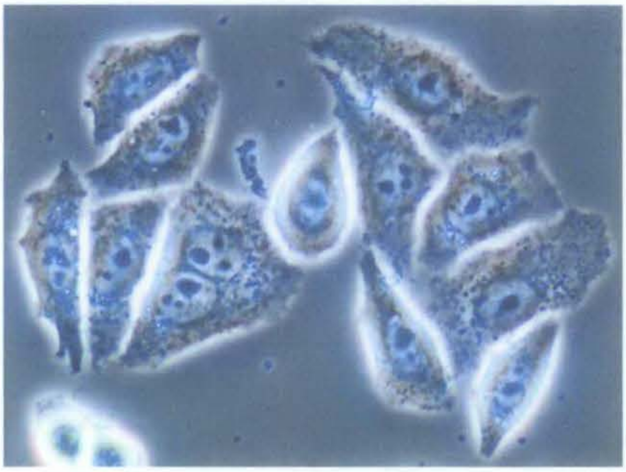

Figure 6. Hela cell structure

Figure 6 shows the Hela cell structure. Some of the characteristics of Hela cells are these cells are adherent cells meaning that they will stick to the cell culture flask, the replication or doubling time is 23 hours and Hela cells can easily contaminate other cell lines as it's often difficult to control. In terms of physical characteristics, the cell size is approximately 2,000 μm^3 in volume and the adherent cell on a slide is 20 μm diameters for 100,000 cells in a confluent well of a 96 multiwell plate. For cell manipulation purpose, it is recommended that the manipulator is capable of grasping each individual cell with actuator displacement of 1 μm during closing to avoid damaging the cell. This requirement will be used in the design of the proposed electrostatic micro actuator system.

CHAPTER 3: METHODOLOGY

3.1 Project Process Flow

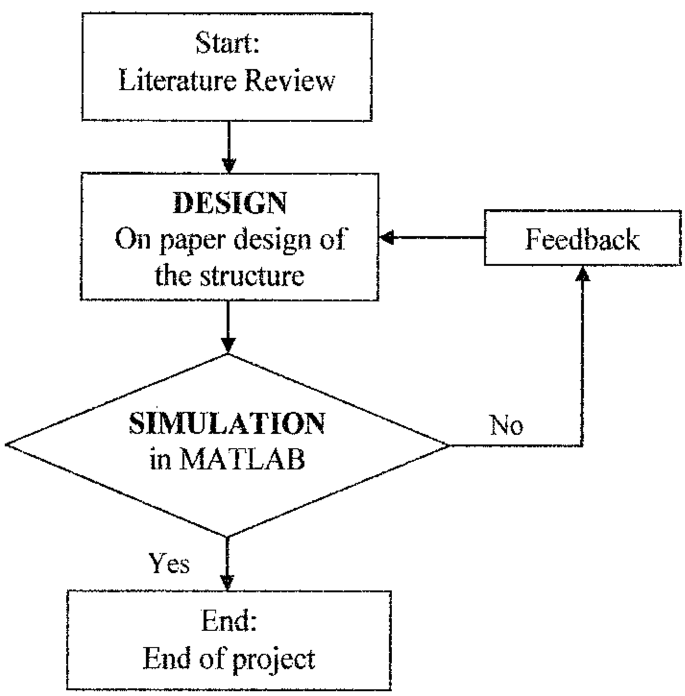

Figure 7. Project flow diagram

In this project, the basic knowledge of actuators using electrostatic principles must be understood prior to designing the structure of the devices starts. Few references showed the examples of microactuator available at the market. After complete designing the devices, the project then is proceed by simulating the performance of the actuators using MATLAB software. The simulation results will be gathered and the optimization of the device will be performed. The feedback of the design structure with simulation result will be analyzed and the error will be calculated.

3.2 Design Structure

Before starts designing, the input and output of the system should be determined in order to view some relations between them. In this case, the actuator voltage, V and current through the comb fingers, I are the inputs of the actuator system. Basically, when the input is given to the actuators, the output from the actuation system should be noted. Therefore, the desired outputs are the electrostatic force produced by the capacitor, F that resulting the displacement of the end of gripper, x and as shown in below.

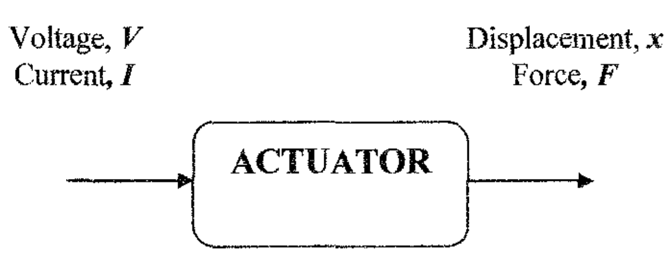

Figure 8. The input-output relation

Before a gripper can be made, the specimen that wanted to be manipulated should be taken into account. For this project, by focusing on the Hela cells manipulation, the size of the Hela cell should be the reference in designing the actuator to avoid photo damage of the cell during manipulation process. Research shows that the stiffness of Hela cell should be $8.38\text{x}10^{-7}$ Nm^{-1} [44]. With estimation of gripping depth applied onto the cell during manipulation is 1 μm, the gripping force experienced by the Hela cell will be 0.84 pN. This is one of the criteria that should be fulfilled in designing the device. Therefore, in order not to harm the cell, the force at gripper arm should be less than the resonant force of Hela cell. As mentioned earlier, the size of Hela cell that need to take into consideration in gripping them is 20 μm. In this case, in order to hold the cell, the gripper should be able to open the end-gripper at least 1 μm. This value will be the second reference of the design device.

3.3 Tools and Equipment required

3.3.1 MATLAB R2007a

The software will be the main tool for developing the simulation of the micrometer design in due to its user friendly interface and the amount of resources available.

CHAPTER 4: MICROACTUATOR DESIGN

This chapter covers the design of the electrostatic based microgripper device that is suitable for Hela cell manipulation. The Microactuator Design consists of the the structure design and also equations used to predict device performance. CMOS-MEMS electrostatic based microactuator is designed based on MIMOS 0.35μm CMOS technology. Based on literature review, to operate the microactuator, the microactuator must be able to operate with gripping depth and force as listed in Table 1 below.

Table 1. Desired microactuator output

Criteria	Value	Unit
Gripping depth	1.0	μm
Gripping force	0.084	pN

4.1 Microactuator Design

Comb finger and dual end-gripper operation are used in this project. The advantage of using the comb finger structure is its ability to resonate, which allows relatively high displacements for corresponding small inputs. The device structure consists of two cantilever beams, two pairs of flexures to support the beam and also comb fingers that form a parallel plate of capacitors. When actuator voltage is supplied through the two parallel plates of capacitor, an electrostatic force will be produced which pull the two plates (rotor and stator) closer. The parallel plates of capacitor are arranged in alternately with opposite sign of polarity. The illustration of comb fingers is illustrated in Figure 9.

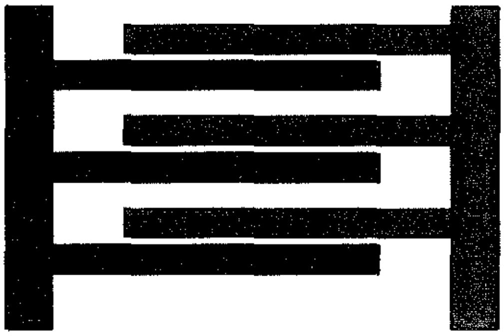

Figure 9. Comb finger illustration (top view)

The combination of certain numbers of parallel plates may produce certain amount of electrostatic force that sufficient for the gripper to move to the desired displacement value. In capacitive part, the parameters that influenced the desired output are the number of parallel plates, *N,* the thickness of the comb finger, *t* and the distance between two parallel plates, *d.* Despite, the air permittivity between the comb fingers should be taken into consideration. Therefore, the calculation to find the electrostatic force, F_e is measured using the equation 4.1.1 as

$$F_e = n\varepsilon\frac{tV^2}{d}. \qquad (4.1.1)$$

After the electrostatic force being calculated, the springs that attached to the flexure beams are also calculated to see the flexibility of the design. For this microactuator, the springs are attached at the beginning of the device and at the end of gripper arms so as to hold and preserve the micron-cells size. The illustration in Figure 10 shows how the springs are attached to the device structure.

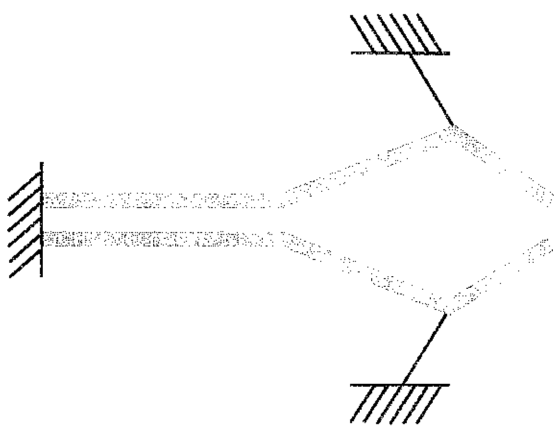

Figure 10. Springs attachment

The springs constant can be determined using Equation (4.1.2) as

$$k = \frac{F}{x} = \frac{6EI}{l^3} = \frac{Et^3w}{2l^3}. \tag{4.1.2}$$

In order to measure the springs constant, the parameters that should be determined are the flexures width, w, flexures thickness, t, and length of the flexures, l. In spite of that, the Young Modulus of 165 GPa is used to specify the flexibility of the springs.

For a normal pair of parallel plates, the resistive force to the plate moving normally against the stationary plate is caused by the damping pressure between the two plates. The damping pressure consists of two main components: the component to cause the viscous flow of air when the air is squeezed out of (or sucked into) the plate region and that to cause the compression of the air film. Therefore, the force component related to the viscous flow is referred to as the viscous damping force, and the force component related to the air compression is referred to as the elastic damping force. If the plate oscillates with a low frequency, or, the plate moves with a slow speed, the gas film is not compressed appreciably. In this case, the viscous damping force dominates. It will be seen later that the viscous force is directly proportional to the speed of the plate.

On the other hand, if the plate oscillates with a very high frequency, or moves with a high speed, the gas film is compressed but fails to escape. In this case, the gas film works like a bellows. Thus, the elastic force dominates. Obviously, the elastic force is directly proportional to the displacement of the plate.

The squeeze damping ratio is then calculated in order to get the dynamic equation of the device. The value of squeeze damping ratio can be measured using this formula:

$$b = \frac{7.2N\mu l w^3}{g^3} \tag{4.1.3}$$

Where μ is the viscosity of the air, N is the number of comb fingers, w is the width of capacitor plate, g is the air gap and l is the length of the capacitor plate. With these information, a microactuator was designed using all the specifications given. The structure of the device can be seen in different angles as shown in the Figure 11 and Figure 12.

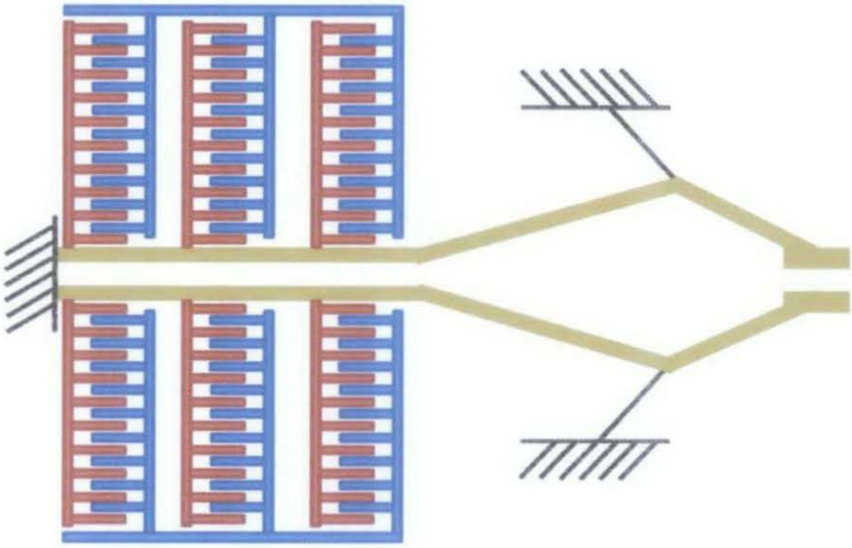

Figure 11. 2-Dimension of electrostatic microactuator structure

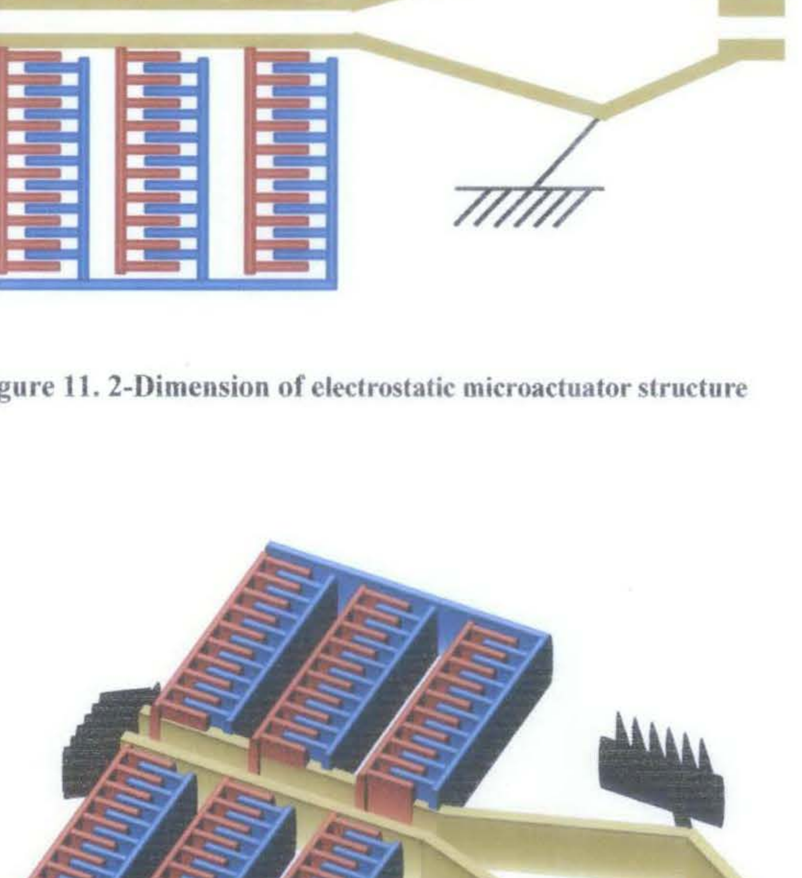

Figure 12. 3-Dimension of Electrostatic microactuator

After few trials and error in optimizing the real value of design structure, all the parameters are then determined. The detailed design is listed in Table 2.

Table 2. Dimension of the electrostatic microactuator

Parameter	Symbol	Value	Unit
Number of capacitors	N	150	-
Thickness of a comb finger	t	5	µm
Width of a comb finger	w	1	µm
Length of a comb finger	l	24	µm
Distance between comb fingers	d	3	µm
Gap of the fingers	d_o	9	µm
Length overlap finger	l_o	18	µm
Gap between gripper jaws	x_o	20	µm
Spring length	l_s	100	µm
Spring thickness	t_s	50	µm

Spring width	w_s	3	μm
Silicon density	ρ_{Si}	2330	Kg/m^3
Silicon Young's modulus	E_{Si}	165	GPa
Aluminum density	ρ_{Al}	2700	Kg/m^3
Permittivity of air	ε_0	8.85×10^{-12}	F/m

CHAPTER 5: RESULTS & DISCUSSION

This chapter discusses on the results obtained from this project. There are two main sections which are simulation results of the optimized structure and also the optimization process results. Both are simulated using MATLAB software.

5.1 Simulation Results of the Structure

All the optimized parameters were listed in Table 3. They were calculated using the formula attached in Chapter 4 and the graphs are analysed. However, the desired displacement of 1 μm is still maintained.

Table 3. Parameters of the result

Parameter	Values	Unit
Mass production, *m*	0.0585	nkg/m^3
Spring constant, *k*	27.844	N/m
Squeeze damping ratio, *b*	0.0444	nNs/m^2
Electrostatic force, F	10.23	μN
Actuated voltage, *V*	68	V
Number of fingers, *N*	150	-

The equations then simulated in MATLAB R2010a to produce the following results on how each changes in actuator voltage supplied will affect the electrostatic forces produced for the gripper to open the jaw of the actuator.

From the results, we found that the sensitivity of the displacement of the device that the total numbers of comb fingers pairs are suitable for this structure by referring to other structures that based their results on the values of micro ranges. The simulation was done step by step to find the relations between the parameters as the input and the mechanical outcome as the output of the device.

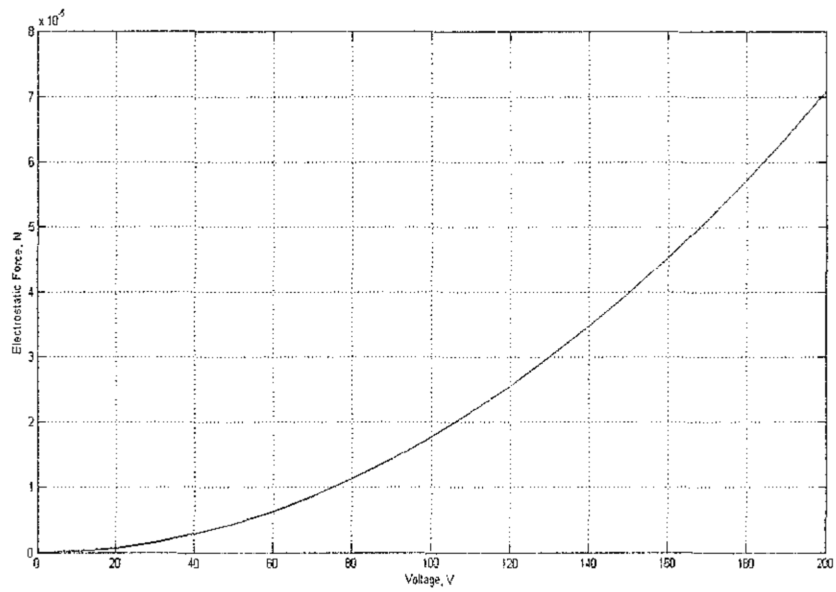

Figure 13. Graph of Electrostatic Force versus Voltage

Based on the graph in Figure 13, the relationship between actuator voltage and the electrostatic force produced by 150 pairs of capacitor is analyzed. For the range of 0 - 200 V supplied to the systems, the electrostatic force experienced by the actuator will be in the range of $0 - 8 \times 10^{-4}$ N.

From the graph, we can say that as the actuator voltage increases, the electrostatic force increases. The graph looks like a positive part of quadratic curve due to the equation used as in the Equation (4.1.1). A MATLAB coding was run in order to get the sensitivity of the structure. The sensitivity of the graph is found to be

4.6 x 10^{-7} N/V. Therefore, we can conclude that for every 1 V supply to the capacitor, 4.6 x 10^{-7} N of electrostatic force was produced.

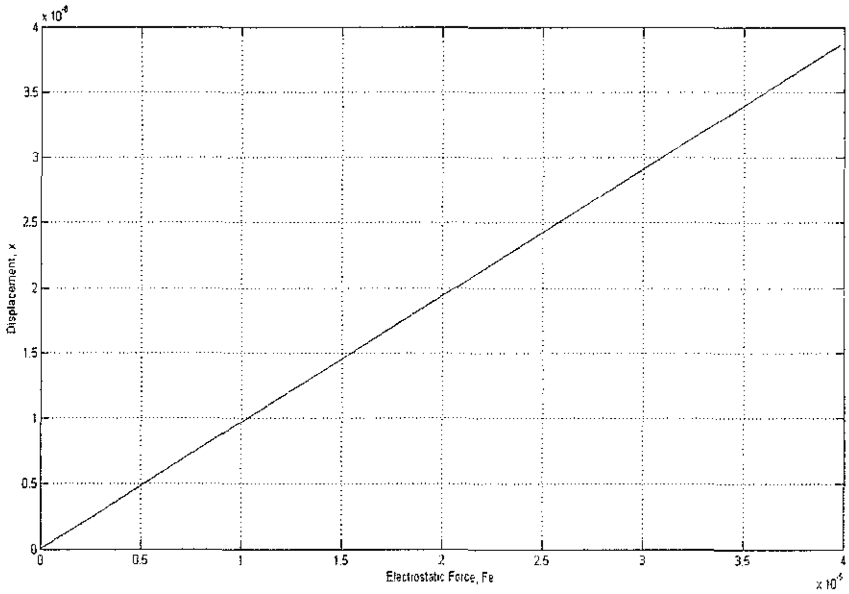

Figure 14. Graph Displacement versus Electrostatic Force

The other analysis was the displacement versus electrostatic force. Based on the graph in Figure 14, the relationship between the electrostatic force produced and the resulting displacement at the end of the gripper arms are shown. For the range of 0 – 40 μN of electrostatic force produced onto the systems, the displacement experienced by the gripper arms will be in the range of 0 – 4 μm.

From the graph, we can conclude that as the electrostatic force increases, the displacement also increases. The graph showed they are directly proportional as in the Equation (4.1.2). A MATLAB coding was run in order to get the sensitivity of the structure. The sensitivity of the graph is found to be 0.09699 N/m. Therefore, to have 1 μm of displacement at the end of the gripper, 10.32 μN of electrostatic force should be produced.

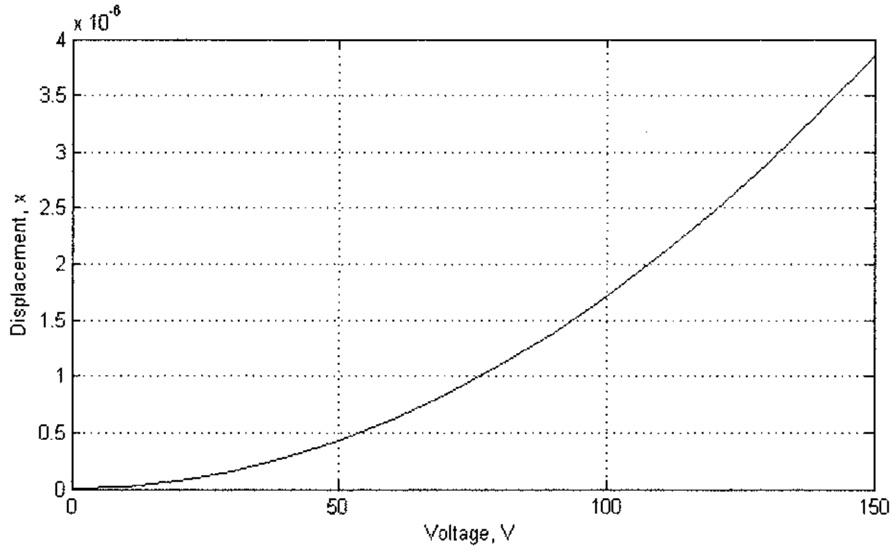

Figure 15. Graph Displacement versus Voltage

The displacement versus the applied voltage was also investigated. Based on the graph in Figure 15, the relationship between the actuator voltage supply and the resulting displacement at the end of the gripper arms are shown. For the range of 0 – 150 V of actuator voltage supply onto the systems, the displacement experienced by the gripper arms will be in the range of 0 – 4 µm.

From the graph, we can say that as the voltage supply increases, the displacement is also increases. The graph looks like a positive part of quadratic curve due to the equation used as in the combination of Equation (4.1.1) and Equation (4.1.2). A MATLAB coding was run in order to get the sensitivity of the structure. The sensitivity of the graph is 3.26×10^{-8} V/m. Therefore, we can say that every 1 V voltage supply, it is resulting 0.0326 µm of displacement at the end of the gripper.

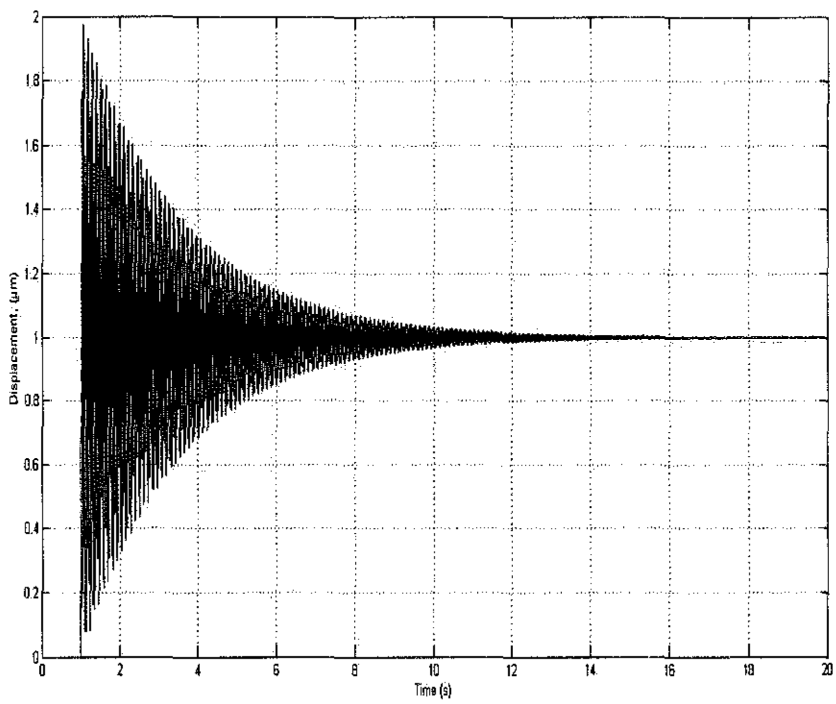

Figure 16. Dynamic in time response function

Next, the dynamic response of the actuator was analyzed. Based on the graph in Figure 16, we can see how the reactions of the device dynamically in time response function. The graph showed that the system is not stable by referring to the oscillatory output between 1 – 14 seconds. The time taken for the system to be stable (or settling down) is approximately 14 – 15 seconds, as we take displacement of 1µm as the reference input.

However, the frequency of the arms to be in initial position can be improved. This process will help the cell manipulation can be done in a short period of time. Some of the parameters listed can be manipulated in order to get the best output.

5.2 Simulation Results of the Optimization Process

Optimization process is done after we simulate the possible parameters that suit the criteria of the devices. After reviewing some results, especially the system dynamic, we can clearly see the stability of the device. That is the reason why optimization should be done in order to get the best output as an improvement for the device.

In order to optimize the device, first of all, we increase the number of comb fingers, *N*. This parameter will affect the device performance in achieving the objectives. As for now, the comb fingers used are 150 pairs, when this number were increasing to 200 pairs, we will see the electrostatic force and voltage required to maintain the displacement.

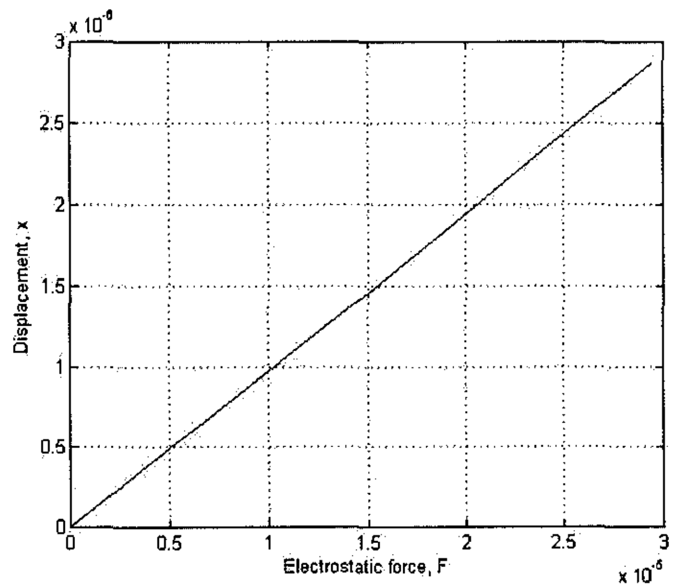

Figure 17. Graph of Displacement versus Electrostatic force with increasing N

By maintaining our goal of having 1μm displacement, and with more comb finger pairs, the electrostatic force needed is approximately 10 μN. Therefore, we can say that when more parallel plates were used, the more electrostatic force was produced to move. Since we have lots of comb fingers, the affect of varying actuator voltage supply to the systems, as illustrated in Figure 18.

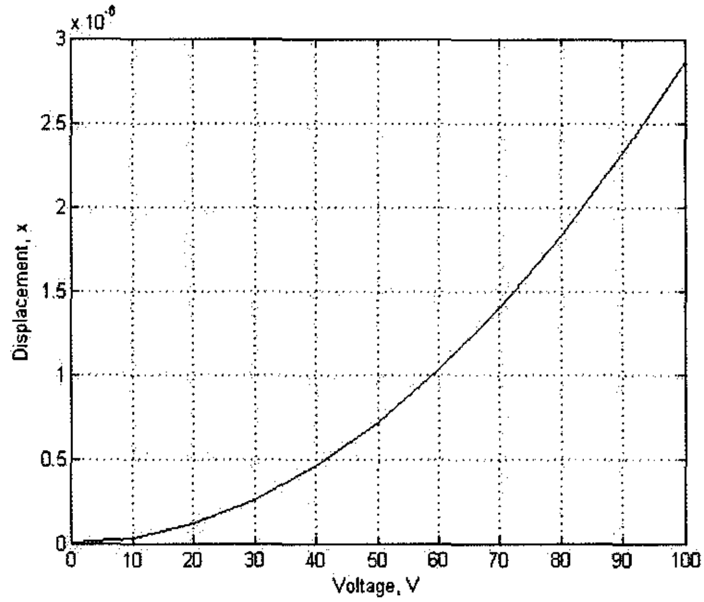

Figure 18. Graph of Displacement versus voltage with increasing N

As for the device performance before, with 150 pairs of parallel plates, only 68 V actuator voltages are required to meet the objectives. When optimization process was done, it shows that if the number of capacitor increasing to 200 pairs, the actuator voltage should be 58 V.

The conclusion for this is increasing number of comb fingers will increase in electrostatic force, and thus the actuator voltage should be reduced in order to have a fixed displacement of 1 μm at the end of the gripper. In addition, it is an advantage for a device to operate in low voltages as this still has the same output that we want.

When we increase the number of parallel plate, N, the squeeze damping ratio, b will also increase by referring to the equation (4.1.3). The numbers of comb fingers are directly proportional to the squeeze damping ratio. As the ratio is related to the dynamic of the device, the changes of the performance was plotted.

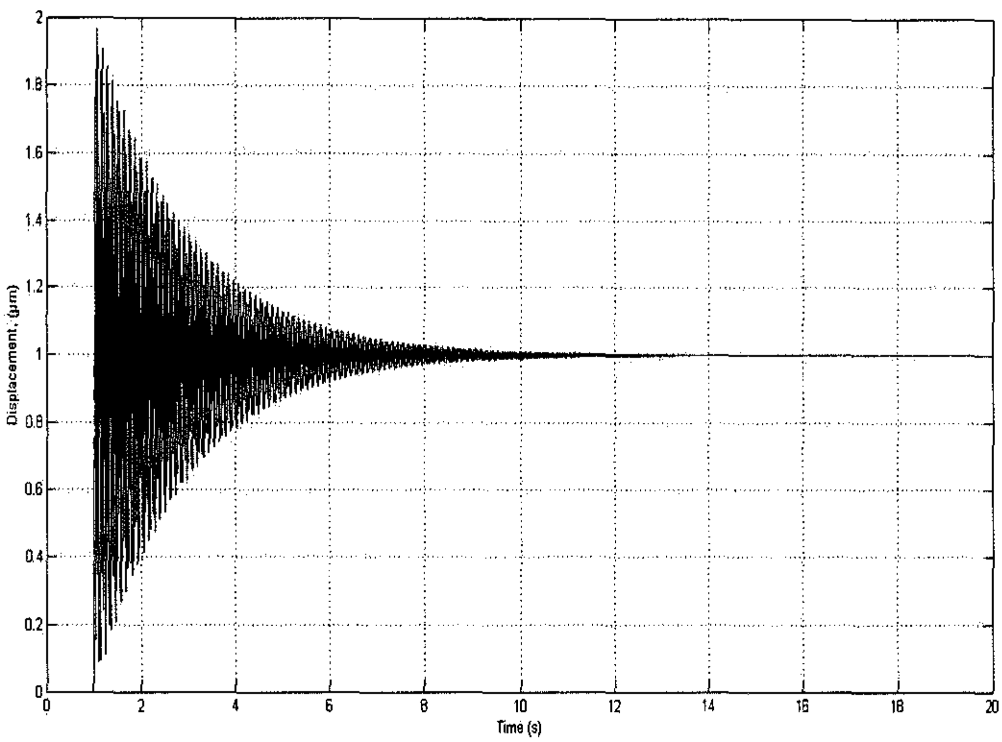

Figure 19. Dynamic system of microactuator with increasing damping ratio, *b*

Figure 19 shows the system dynamic after the effect of increasing number of fingers thus increase the damping ratio. These changes affect the system stability. The system is less oscillatory and time taken for the system to be stable is approximately 11second.

The system should have less settling time and overshoot. As for this case, the dynamic is better than the one in Figure 16. In order to improve the system dynamically, the value of spring constant is changed to see their performance.

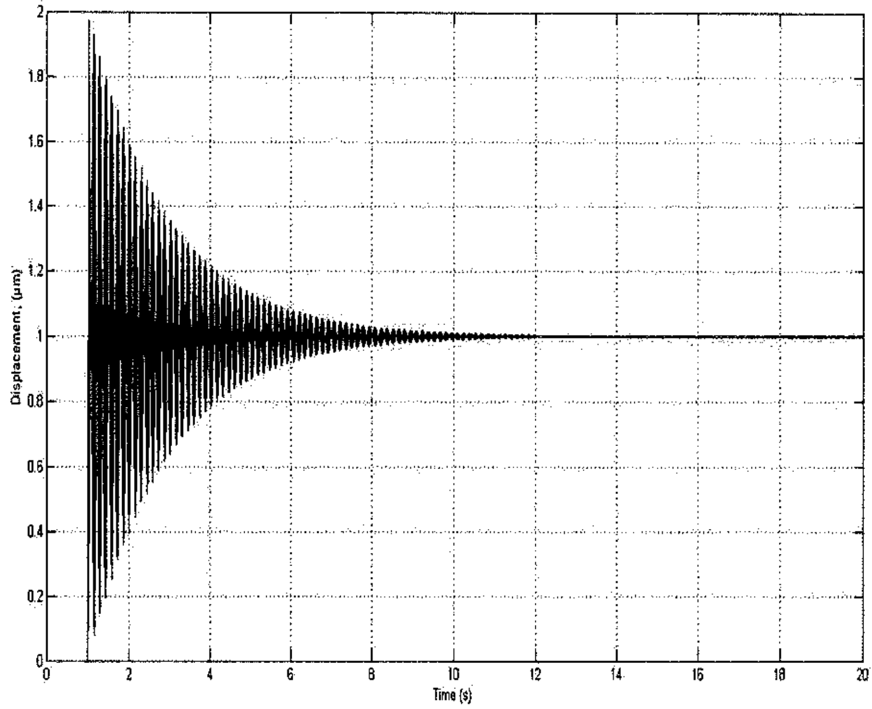

Figure 20. Dynamic system of microactuator with decreasing constant, *k*

The dynamic of the microactuator for this project with decreasing constant, *k* can be seen in Figure 20. To decrease the value of spring constant, we may increase the length of the spring, *l*, and the width of the beam, *w*. The equation used for this part is equation (4.1.2).

To compare, there is little difference in the oscillatory pattern from the previous one. It is less oscillatory compared to the graph in Figure 19. However, time taken for the actuator to be at initial position is still at 11 seconds. The optimized parameters are listed in Table 4.

Table 4. Optimized parameters

Parameter	Values	Unit
Mass production, *m*	0.0585	nkg/m^3
Spring constant, *k*	7.7344	N/m
Squeeze damping ratio, *b*	0.0592	nNs/m2
Electrostatic force, F	9.9238	μN
Actuated voltage, *V*	58	V
Number of fingers, *N*	200	-

CHAPTER 6

CONCLUSION AND RECOMMENDATIONS

6.1 Conclusion

By researching the characteristics of Hela cells and technology in MEMS family, we decided in designing a microactuator using the electrostatic principle for biomedical use. Basically, the electrostatic based microactuator uses numbers of comb-drive parallel plate with potential difference and motion produced an electrostatic field.

The ability of the microactuator is they manage to grip the cell with 1 μm displacement and supply 0.084 pN gripping force onto the cell. From the results, we can say that the gripper use low voltage which is 58 V and 9.9238 μN of electrostatic force to get displacement of 1 μm. Other than that it has settling time of 11 seconds.

The device is optimized by increasing the number of comb fingers, *N,* then resulting the increasing of squeeze damping ratio, *b.* The system is still unstable with less settling time. Logically, the springs that support the beam should be decreased in order to have suitable spring length, *l.*

6.2 Recommendations

There are a few recommendations that can be done to improve this project:

- Varying the variables number of fingers, spring constant and the damping ratio.
- Simulate the design structure using dedicated ConventorWare software to clearly see the device performance mechanically.

REFERENCES

[1] James J. Paulsen, Joseph M. Giachino, " Powertrain Sensors and Actuators: Driving Toward Optimized Vehicle Perormance", pp. 575.

[2] Hartmut Janocha, "Microactuators", *Actuators: basics and principle*, Springer 2004, pp. 320.

[3] Jacek F. Gieras, "Microelectromechanical system", *Advancements in electric machines,* Springer 2008, pp. 13.

[4] B.A Parviz, T.-K Allen Chou, C. Zhang, K. Najafi, M.O. Muller, P.D Washabaugh, L.P. Bernal, "Performance of ultrasonic electrostatic resonators for use in micro propulsion," *The 14th IEEE International Conference on Micro Electro Mechanical Systems, Interlaken Switzerland 2001*, pp. 586-589.

[5] G. Galambos, et al., "A Surface Micromachined Electrostatic Drop Ejector," Proceedings of transducers '01. *11th Conference on Solid- State Sensors and Actuators, Munich, Germany,* June 10-14, 2001, pp. 906-909.

[6] S. Kamisuki, et al., "A High Resolution, Electrostatically Driven Commercial Inkjet Head," Proceedings of MEMS'00, *13th IEEE Workshop on Micro Electromecanical System, Miyazaci Japan*, Jan.23- 27, 2000, pp. 793-798.

[7] Gary Sunada, "MicroElectroMechanical (MEMS)", *START: Selected Technology Assurance Research Technology*, 2001 Volume 8, Number 1, pp. 1.

[8] Biyovraj Sahu, Curtis R. Taylor, Kam K. Leang, "*Emerging Chalengges of Microactuators for Nanoscale positioning, Assembly, and Manipulation*", 21 August 2010.

[9] Sardan, O., Eichhorn, V., Petersen, D. H., Fatikow, S., Sigmund, O., and Boggild, P., 2008, "Rapid Prototyping of Nanotube-Based Devices Using Topology-Optimized Microgrippers," Nanotechnology, 19(49), p. 495503.

[10] Kimberly, T., Matthew, E., Aaron, G., George, S., and Phil, F., 2004, "FIB Prepared TEM Sample Lift-Out Using MEMS Grippers," Microsc. Microanal., 10, (S02), pp. 1144–1145.

[11] Chronis, N., and Lee, L. P., 2005, "Electrothermally Activated SU-8 Microgripper for Single Cell Manipulation in Solution," J. Microelectromech. Syst., 14(4), pp. 857–863.

[12] Kim, K., Liu, X., Zhang, Y., and Sun, Y., 2008, "Nanonewton Force-Controlled Manipulation of Biological Cells Using a Monolithic MEMS Microgripper With Two-Axis Force Feedback," J. Micromech. Microeng., 18(5), p. 055013.

[13] Requicha, A. A. G., 2003, "Nanorobots, NEMS, and Nanoassembly," Proc. IEEE, **9**, pp. 1922–1933.

[14] B. E. Volland et al., "Electrostatically driven microgripper", Microelectron. Eng 61/62 (2002), pp. 1015-1023.

[15] I. P. F. Harouche and C. Shafai, "Simulation of shaped comb drive as a stepped actuator for microtweezers application", Sens. Actuators, A 123-124 (2005), pp. 540-546.

[16] RD Isaac, "*The Future of CMOS Technology*", IBM Journal of Research and Development, 2000, pp 1 – 3.

[17] Baker, R. Jacob (2008). *CMOS: circuit design, layout, and simulation* (Second ed.). Wiley-IEEE. p. xxix.

[18] Mikael Sterner, "*Numerical Algorithms and their Application to MEMS Electrostatic Actuators*", Master's Degree Project in Electrical Measurement Technology, 2006, pp 3 – 4.

[19] Hiroki Morimura, Shinichiro Mutoh, Hiromu Ishii, Katsuyuki Machida, "Integrated CMOS-MEMS Technology and Its Applications", *9th International Conference,* pp. 2460 – 2463.

[20] R.H. Grace, "Semiconductor Sensors and Microstructures in Automotive Applications, Sensors and Actuators", *Society of Automotive Engineers International Conference Proceedings*, 1991, pp. 245-260.

[21] F. Najar, "Static and Dynamic Behaviour of MEMS Microactuators", *National Engineering School of Tunisia*, 2008, pp. 7-8.

[22] Y. Nemirovsky and O. Bochobza-Degani, "A methodology and model for the pull-in parameters of electrostatic actuators," *Journal of Microelectromechanical Systems*, vol. 10, no. 4, pp. 601–615, December 2001.

[23] E. S. Hung and S. D. Senturia, "Extending the travel range of analog-tuned electrostatic actuators," *Journal of Microelectromechanical Systems*, vol. 8, no. 4, pp. 497–505, December 1999.

[24] C.H. Mastrangelo, M.A. Burns, and D.T. Burke, "Microfabricated devices for genetic diagnostics," *Proc.. IEEE,* 86(8):1769-1787 (1998).

[25] M.U. Kopp, A.J. de Mello, and A. Manz, "Chemical amplification: continuos-flow PCR on a chip," *Science*, 280: 1046-1048 (1998).

[26] M.A. Northrup, M.T. Ching, R.M.White, and R.T. Watson, "DNA amplification with a microfabricated reaction chamber," *Proc. Int. Conf. Solid-State Sensors and Actuators (Tranducers 93),* June 1993, pp. 924-926.

[27] E.T. Lagally, P.C. Simpson, and R.A. Mathies, "Monolithic integrated microfluidic DNA amplification and capillary electrophoresis analysis system," *Sensors and Actuators B*, 63: 138-146 (2000).

[28] J.R. Webster, M.A. Burns, D.T. Burke and C.H. Mastrangelo, "Monolithic capillary electrophoresis device with integrated fluorescence detector," *Anal. Chem.*, 73: 1622-1626 (2001).

[29] M.A. Burns, B.N. Johnson, S.N. Brahmasandra, K. Handique, J.R. Webster, M. Krishnan, T.S. Sammarco, P.M. Man, D. Jones, D. Heldsinger, C.H. Mastrangelo and D.T. Burke, "An integrated nanoliter DNA analysis device," *Science*, 282: 484-487 (1998).

[30] R.H. Carlson, C.V. Gabel, S.S Chan, R.H. Austin, J.P. Brody and J.W. Winkelman, "Self-sotting of white blood cells in a lattice," *Phys. Rev. Lett.*, 79(11): 2149-2152 (1997).

[31] T.A.J. Duke and R.H. Austin, "Microfabricated sieve for the continous sorting af macromolecules," *Phys. Rev. Lett.*, 80(7): 1552-1555 (1998).

[32] J.T. Santini, Jr., M.J. Cima and R. Langer, "A controlled-release microchip," *Nature*, 397: 335-338 (1999).

[33] S. Henry, D.V. McAllister, M.G. Allen and M.R. Prausnitz, "Micromachined needles for the transdermal delivery of drugs," *Proc. IEEE MEMS 1998*, pp. 494-498.

[34] S. Hashmi, P. Ling, G. Hashmi, M. Reed, R. Gaugler and W. Trimmer, "Genetic transformation of nematodes using arrays of micromechanical piercing structures," *BioTechniques*, 199: 766-770 (1995).

[35] M.L. Reed, C. Wu, J. Kneller, S. Watkins, D.A. Vorp, A. Nadeem, L.E. Weiss, K. Rebello, M. Mescher, A.J. Conrad Smith, W. Rosenblum and M.D. Feldman, "Micromechanical devices for intravasculardrug delivery," *J. Pharma. Sci.*, 8(11): 1387-1394 (1998).

[36] A. Trautman, P. Ruther and O.Paul, "Microneedle arrays fabricated using suspended etch mask technology combined with fluidic through wafer bias" *Proc. MEMS 2003*, Kyotot, Japan, Jan. 2003, pp. 682-691.

[37] P. Griss and G. Stemme, "Novel, side opened out-of-plane microneedles for microfluidic transdermal interfacing," *Proc. MEMS 2002*, Las Vegas, USA, Jan. 2002, pp. 467-470.

[38] J.G.E. Gardeniers, J.W. Berenschot, M.J. de Boer, Y. Yeshurun, M. Hefetz, R. van't Oever and A. van den Berg, "Silicon micromachinedhollow microneedles for transdermal liquid transfer," *Proc. MEMS 2002*, Las Vegas, USA, Jan. 2002, pp. 141-144.

[39] R. Dizon, H. Han, A. G. Russell and M. L. Reed, "An ion milling pattern transfer technique for fabrication of three-dimensional micromechanical structures," *J. Microelectromechanical Systems*, 2(4): 151-159 (1993).

[40] M. Esashi, "Micro elcetro mechanical systems by bulk silicon micromachining," *Proc. 2nd Int. Symp. Microstructures and Microfabricated Systems*, Electrochem. Soc. (1995), pp. 11-23.

[41] A.E. Guber, N. Giordano, A. Schüslsler, O. Baldinus, M. Loser and P. Wieneke, "Nitinol-based microinstruments for endoscopic neurosurgery," *Actuator 96, 5th Int. Conf. New Actuators* (1996), pp. 375-378.

[42] T. A. Desai, D.J. Hansford, L. KUlinsky, A. H. Nashat, G. Rasi, J. Tu, Y. Wang, M. Zhang and M. Ferrari, "Nanopore technology for biomedical applications," *J. Biomed. Microdevices,* 2(1): 11-40 (1999).

[43] L. Leoni, and T.A. Desai, "Biotrasport and biocompatibility of nanoporous biocaplsules," *1st Ann. Int. IEEE-EMBS Special Topic Conf. on Microtechnologies in Medicine & Biology* (2000), pp. 113-117.

[44] NEALE Steven L., OHTA Aaron T., HSU Hsan-Yin, VALLEY Justin K., JAMSHIDI Arash, WU Ming C., "Force versus position profiles of HeLa cells trapped in phototransistor-based optoelectronic tweezers", *Emerging digital micromirror device based systems and applications*, San Jose CA , ETATS-UNIS (2009) 2009 , vol. 7210 [Note(s) : 1 vol.,].

APPENDIX I : MATLAB CODES

Voltage vs. Capacitive Force

```
n = 200;
e = 8.85e-12;
t = 5e-6;
d = 3e-6;
v = 0:10:150;
F = ((n*e*t*(v.^2))/d);
plot(v,F);
xlabel('Voltage, V');
ylabel('Electrostatic Force, N');
grid on;
```

Displacement vs. Capacitive Force

```
v = 68;
e = 8.85e-12;
t = 5e-6;
d = 3e-6;
n = 0:10:200;
F = ((n*e*t*(v^2))/d);
s = 50e-6;
E = 1.65e11;
w = 1e-6;
l = 100e-6;
k = (E*w*(s^3))/(2*(l^3));
x = F/k;
plot(F,x);
xlabel('Electrostatic Force, Fe');
ylabel('Displacement, x');
grid on;
```

Displacement vs. Voltage

```
n = 150;
e = 8.85e-12;
t = 5e-6;
d = 3e-6;
v = 0:10:100;
F = ((n*e*t*(v.^2))/d);
E = 1.65e11;
w = 1e-6;
l = 100e-6;
ws= 3e-6;
ts= 50e-6;
k = (E*ws*(ts^3))/(2*(l^3));
x = F/(2*k);
plot(v,x);
xlabel('Voltage, V');
ylabel('Displacement, x');
```

Dynamic of the systems

```
m = 5.8534e-11;
k = 7.7344;
b = 5.9195e-11;
A = [0          1
    -k/m       -b/m];
B = [0
    1/m];
C = [1  0];
D=0;
T = 0:0.01:20;                  % simulation time = 10 seconds
U = [zeros(1,100),ones(1,length(T)-100)];          % no input
Y = lsim(A, B, C, D, U, T);    % simulate and plot the response (the
output)
plot(T,Y);                      % plot the output vs. time
grid on;
```